IEEE Access
Multidisciplinary | Rapid Review | Open Access Journal

Received 30 September 2024, accepted 4 December 2024, date of publication 12 December 2024,
date of current version 30 December 2024.

Digital Object Identifier 10.1109/ACCESS.2024.3516520

RESEARCH ARTICLE

Amputee Gait Phase Recognition Using Multiple GMM-HMM

WENYAO ZHU[1], (Graduate Student Member, IEEE), ZHENBANG LIU[1], YIZHI CHEN[1], DEJIU CHEN[2], (Senior Member, IEEE), AND ZHONGHAI LU[1], (Senior Member, IEEE)

[1]Department of Electrical Engineering, KTH Royal Institute of Technology, 114 28 Stockholm, Sweden
[2]Department of Engineering Design, KTH Royal Institute of Technology, 114 28 Stockholm, Sweden

Corresponding authors: Dejiu Chen (chen@md.kth.se) and Zhonghai Lu (zhonghai@kth.se)

This work was supported in part by the Research Project SocketSense, funded by the European Union's Horizon 2020 Research and Innovation Program under Grant 825429.

This work involved human subjects or animals in its research. Approval of all ethical and experimental procedures and protocols was granted by Comité de Ética de la Investigación con medicamentos (CEIm) and Agencia Española de Medicamentos y Productos Sanitarios (AEMPS) in Spain, and Health Research Authority (HRA) and Medicines and Healthcare Products Regulatory Agency (MHRA) in U.K. (IRAS Project ID: 292614).

ABSTRACT Gait analysis helps clinical assessment and achieves comfortable prosthetic designs for lower limb amputees, in which accurate gait phase recognition is a key component. However, gait phase detection remains a challenge due to the individual nature of prosthetic sockets and limbs. For the first time, we present a gait phase recognition approach for transfemoral amputees based on intra-socket pressure measurement. We proposed a multiple GMM-HMM (Hidden Markov Model with Gaussian Mixture Model emissions) method to label the gait events during walking. For each of the gait phases in the gait cycle, a separate GMM-HMM model is trained from the collected pressure data. We use gait phase recognition accuracy as a primary metric. The evaluation of six human subjects during walking shows a high accuracy of over 99% for single-subject, around 97.4% for multiple-subject, and up to 84.5% for unseen-subject scenarios. We compare our approach with the widely used CHMM (Continuous HMM) and LSTM (Long Short-term Memory) based methods, demonstrating better recognition accuracy performance across all scenarios.

INDEX TERMS Gait phase recognition, Gaussian mixture model, hidden Markov model, lower limb prosthesis.

I. INTRODUCTION

There are approximately 40 million amputees worldwide and the number is expected to increase due to an aging population and diseases [1]. Transfemoral patients constitute a substantial part of all amputees [2]. The demand for effective prosthetic socket designs grows rapidly to improve rehabilitation comfort and safety for lower-limb amputees.

One of the main tasks of these prosthesis systems is to ensure the tight coupling between the human limb and the artificial prosthetic socket, especially under dynamic situations [3], [4]. Biomechanical studies have demonstrated significant differences in the human lower limb joint kinematic and kinetic across various locomotion patterns and gait phases [5]. Consequently, the efficacy of prosthesis systems hinges on their ability to perceive leg movements accurately, thereby imposing stringent demands on gait analysis.

The gait analysis based on intra-socket dynamic pressure measurement is a popular approach to assist prosthetists in identifying various impairments during walking [6], [7] and achieve a better fit of the socket [1]. Gait activities can be treated as discrete gait phases in a cycle. Accurate gait phase recognition is a key component of successful gait analysis. Other applications such as the active prosthetic exoskeletons [8], [9], [10] and auto-adjustable socket [11], [12] also need precise gait phase recognition for their control logic.

In recent years, various approaches for gait phase detection have been developed. Most of them are based on wearable sensor measurements including inertial measurement

The associate editor coordinating the review of this manuscript and approving it for publication was Bing Li.

units (IMU), foot switches, electromyography sensors (EMG), and their combinations [13]. However, the existing methods couldn't perform well in the context of intra-socket pressure measurements. Amputee gait phase recognition based on interfacial pressure remains challenging, as the multi-position pressure signals are more complex and less straightforward compared to data from conventional sensor measurements. Natural differences such as the subject's weight, socket size, and walking habits can also affect pressure behaviors.

In this paper, we propose a multiple GMM-HMM (Hidden Markov model with the Gaussian mixture model) approach for amputee gait phase recognition based on the intra-socket pressure measurement.

We summarize our contributions as follows:

- A supervised multiple-GMM-HMM framework is developed for amputee gait phase recognition.
- Our gait phase recognition utilizes the interfacial pressure between the residual limb and socket captured by wearable sensors as features.
- Our approach is evaluated in real amputee gait analysis, where the data come from clinical measurements on human subjects with different conditions.

In the rest of the paper, we discuss the related work in Section II, and the background of GMM-HMM in Section III. Then we define the research problem in Section IV and describe our recognition approach in Section V. Section VI presents the experimental results. We compare our approach with other recognition methods in Section VII and we conclude in Section VIII.

II. RELATED WORK

Intra-socket pressure measurement plays an important role in prosthetic socket designs [14], in which great attention has been paid to gait analysis. Several studies have been conducted on interfacial pressure distributions during gait cycles through physical testing and data modeling [15], [16]. A mechatronics-twin framework [3] enables bio-mechanical simulation of dynamic intra-socket loads along with the gait events for studying operational conditions and revealing anomalies. Recent technological advances focus on automatic assistive devices and self-adjustable sockets [8], [10], [11], [12], [17], where the control parameters also rely on the perception of gait phases and pressure patterns [18]. One major task is accurate gait phase recognition to enhance understanding of gait responses and generalize the measured outcomes.

Conventional gait phase recognition methods usually rely on expert knowledge to reveal the fundamental relationships in gait events. A threshold-based time-frequency analysis method is proposed in [19] for non-disabled human gait phase detection. Maqbool et al. [20] developed a heuristic rule-based amputee gait event detection system using the IMU data. Although these methods report high recognition accuracy, they rely heavily on extensive prior knowledge and labeled data for empirical rule-based decisions, restricting their effectiveness with unencountered samples.

With the development of machine learning technology, artificial neural network-based (ANN) approaches have been applied to gait phase detection. Among these ANN models, the Long Short-term Memory (LSTM) network is a common choice since they are well-suited for sequential data with temporal dependencies. Cai et al. [21] present an EMG-based gait phase recognition method using a variation of the LSTM model. Unfortunately, their method requires healthy subjects so that lower limb surface EMG signals can be obtained, which couldn't be applied to transfemoral amputees. Ding et al. [22] propose a gait phase detection method using a single IMU and an LSTM-based algorithm that can achieve 91.4% accuracy. Tran et al. [23] develop a multi-model LSTM for learning the temporal features of gait using an IMU sensor. They employ six LSTMs, each for processing one channel of the IMU data. Sarshar et al. [24] propose a multiple LSTM method for IMU-based gait analysis. They trained three separate LSTMs, each for estimating one individual gait phase including Toeoff, Midswing, and Heelstrike.

Besides LSTM, HMM and its variants represent another widely used class of machine learning methods for gait pattern recognition. Attal et al. [25] have employed the multiple-regression Hidden Markov model (MR-HMM) using foot plantar pressure for gait phase recognition. However, their focus is on non-amputee individuals, where insole pressure sensors are required for each foot. That is hard to apply to amputees. Later on, they proposed a continuous HMM (CHMM) approach [26] based on two IMUs, which deploys a single GMM-HMM to recognize gait phases. Their approach can learn in an unsupervised manner, but the average recognition rate of 82.47% on the individual subject is not enough for gait analysis. Other popular recognition approaches can be found in [13], but there is no specific method for amputee gait phase recognition concerning interfacial pressure.

GMM-HMM extends the HMM with better recognition ability, as each emission is modeled as a multivariate Gaussian distribution. In [27] and [28], researchers employed GMM-HMM for high-accuracy hand gesture recognition and human activity recognition. Given that interfacial pressure readings and gait events can be treated as sequential observations, GMM-HMM has the potential for amputee gait phase recognition. In this study, we propose a method utilizing multiple GMM-HMM models for accurate amputee gait phase recognition using interfacial pressure data. To the best of our knowledge, this is the first work to address amputee gait phase recognition based on intra-socket pressure measurement.

III. PRELIMINARY ON GMM-HMM

A. HIDDEN MARKOV MODEL

Hidden Markov model (HMM) is a statistical Markov model that generates hidden states from observed sequences. A formal HMM contains three probability parameters $\lambda = (\pi, A, B)$ [29]. Suppose there are n hidden states

$S = \{s_1, \cdots, s_n\}$ in HMM and k distinct observation symbols $V = \{v_1, \cdots, v_k\}$. The state at time t is $q_t \in S$. The observation sequence is $O = \{o_1, \cdots, o_T\}$ with length T, in which each observation o_t is a symbol from V. HMM assumes that the observation at time t only depends on the current hidden state q_t, and the states follow a Markov process.

The initial probability $\pi = [\pi_1, \cdots, \pi_n]$ shows the starting distribution of input at each state. The state transition probability matrix $A = [a_{11} \cdots a_{ij} \cdots a_{nn}]$ indicates how likely the HMM is to transit from the current state to each of the states, in which $a_{ij} = P[q_{t+1} = s_j | q_t = s_i], 1 \leq i, j \leq n$. The emission probability distributions $B = b_i(o_t)$ represent the likelihood of an observation o_t being generated from state s_i. It converts the hidden state path into a sequence of symbols, where the emission probability of each state is modeled by a single Gaussian distribution.

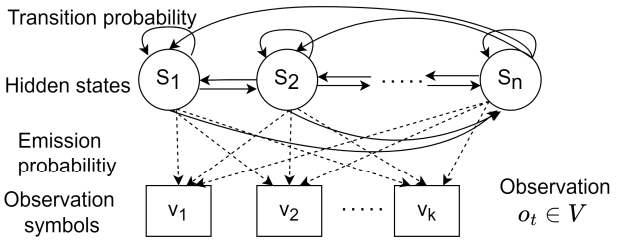

FIGURE 1. An example of a Hidden Markov model.

Fig. 1 shows a typical HMM which finds the most likely symbol for the observed sequence. The learning process aims to estimate the best HMM parameters λ. There are two well-known training methods, the Baum-Welch algorithm, and the Viterbi training [30]. Instead of maximizing the likelihood of the observed data, Viterbi training maximizes the probability of the most likely hidden state sequence [31], which has less complexity.

B. HIDDEN MARKOV MODEL WITH GAUSSIAN MIXTURE MODEL

Hidden Markov model with Gaussian mixture model (GMM-HMM) is a variant of HMM. Instead of one Gaussian distribution per state, the emission distribution is represented as a mixture of multiple multivariate Gaussian densities. The parameters of a GMM with weighted sum of M component densities is $g = (c_m, \mu_m, \Sigma_m), m = 1, \cdots, M$, in which c_m is the mixture weight, μ_m and Σ_m are the mean and covariance matrix of the mth component. Then at state j, the emission probability is calculated by **Eq.** (1).

$$b_j(o_t) = \sum_{m=1}^{M} c_{m,j} \mathcal{N}(o_t | \mu_{m,j}, \Sigma_{m,j}) \tag{1}$$

The Viterbi training procedure [29], [32] of GMM-HMM can be summarized as follows:

1) Each frame of feature vectors is assigned to an HMM state by forced Viterbi alignment [32]. At each state j, $g = (c_{m,j}, \mu_{m,j}, \sigma_{m,j})$ is the Gaussian parameter. The K-means clustering algorithm is used to generate g, where K is set as the number of mixtures.
2) The hidden state corresponding to each observation is obtained. The GMM-HMM parameters are $\lambda = (\pi, A, g)$, which is calculated from the assignment of input over states.
3) Update model parameters as **Eq.** (2), where $C(i)$ represents the number of times that the initial state is s_i, and $C(i \to j)$ is the number of transitions from state s_i to state s_j. g is updated using Viterbi re-estimation [32].

$$\hat{\pi} = \frac{C(i)}{\Sigma_K C(k)}, \quad \hat{a_{ij}} = \frac{C(i \to j)}{\Sigma_K C(i \to k)} \tag{2}$$

4) Repeat steps 2 and 3 until the model is converged. After several iterations, the trained model can be used to make new alignments on the training data.

Based on the trained GMM-HMM, the recognition of newly observed data becomes possible by finding the maximum emission probability of the observation over each state.

IV. PROBLEM DEFINITION

Gait phase recognition is a key requirement for gait analysis. A large amount of complex data on gait activities makes manual gait phase labeling time-consuming and inaccurate. The research problem then focuses on how to perform accurate amputee gait phase recognition using intra-socket pressure measurement.

A. INTRA-SOCKET PRESSURE MEASUREMENT

Since the problem is based on intra-socket pressure measurement, the interfacial pressure is the necessary feature as input and the data collection is described below.

Fig. 2 illustrates the acquisition of intra-socket pressure from multiple sensors mounted on the inner surface of the prosthetic socket. These sensors can be individually placed or connected in the form of a strip or a pad. We show an example of 21 sensors on four strips arranged alongside four socket edges. They can measure pressure between the stump (residual limb protected by liner) and the socket. Each input feature frame represents the reading of all pressure sensors from the same sampling time, then the interfacial pressure is treated as multivariate sequential data. From this, we can observe the cyclical response, which indicates the gait cycles.

External sensors for gait monitoring may cause inconvenience to amputees and prosthetists during clinical tests. Aligning such gait information with current pressure measurements needs extra processing overhead. Therefore, we exclusively rely on the intra-socket pressure for gait phase recognition.

B. GAIT PHASE DESCRIPTION

For amputees, the gait analysis focuses on the periodic leg movement of the amputation side, namely gait cycles. The fundamental division includes Swing (SW) and Stance (ST),

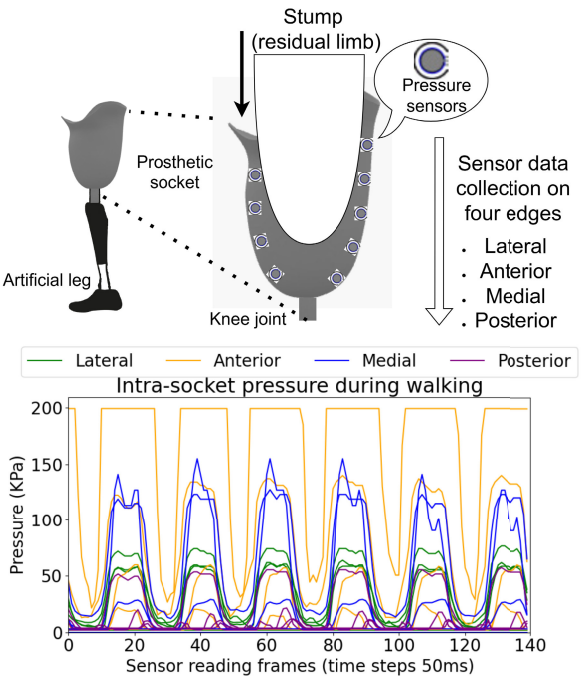

FIGURE 2. Intra-socket pressure data collection.

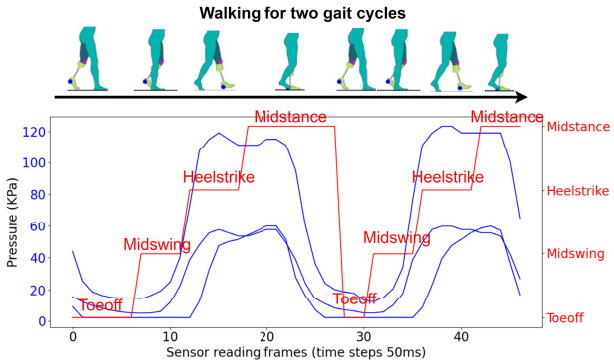

FIGURE 3. The example of four gait phases in the gait cycle.

and there are different granularity of gait phases [33]. To keep generality and synchronize with the clinical assessment, a simplified four-phase model from the classic gait terms [34] is selected, involving Toeoff, Midswing, Heelstrike, and Midstance. **Fig.** 3 shows the four gait phases and the corresponding pressure curves within two consecutive gait cycles.

In particular, Toeoff is the pre-swing state, where the toes leave the ground. Midswing occurs when the foot swings in the air. Heelstrike means the heel is in contact with the ground. During Midstance, the body is supported only by the prosthetic leg. Since the gait phases are not equal in length, our approach should be able to recognize not only long phases but also short phases such as Toeoff.

In our study, we aim to match the pressure sensor readings with actual gait activities accurately. Especially, intra-socket pressure data are given as input that each pressure segment contains I data frames $X = \{x_1, \cdots, x_I\}$. The recognition task is to label them with one of the four gait phases, $L(x_i) \in \{\text{Toeoff, Midswing, Heelstrike, Midstance}\}$, for all $x_i \in X$.

V. GAIT PHASE RECOGNITION METHOD

A. OVERVIEW

We use multiple GMM-HMM for amputee gait phase recognition. **Fig.** 4 shows the proposed method overview. Since the recognition target is four gait phases, the number of GMM-HMM models is set to four. The idea is to learn separate models specified for each gait phase. It runs in a supervised manner. The pressure data are partitioned into the train set and test set. The gait cycles are segmented according to gait phases to create the dataset with ground truth, which serves as the model input.

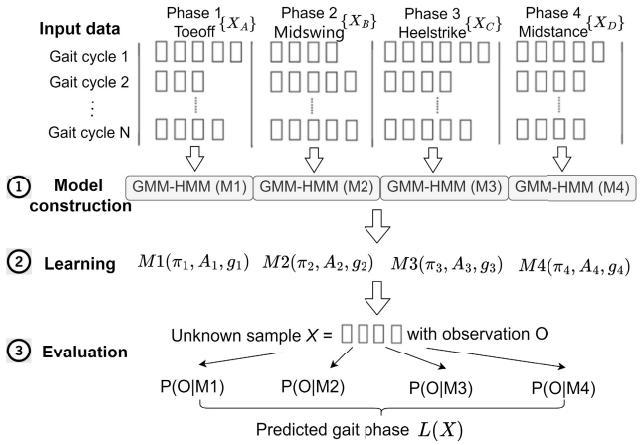

FIGURE 4. Overview of multiple GMM-HMM for gait phase recognition.

Three main processes in **Fig.** 4 are as follows.

1) Model construction: The structure of GMM-HMM is determined by the physical condition of the gait movement. The model parameters $\lambda = (\pi, A, g)$ are initialized based on the input pressure from the train set.
2) Learning: The parameters λ are updated by Viterbi training. The learning step iterates until the model converges.
3) Evaluation: The emission probabilities are obtained on the test dataset from the learned GMM-HMM to predict gait phases. The predicted gait phases are compared with ground truth to find the recognition accuracy.

For each GMM-HMM, the procedure is the same except that they use different input data for learning with respect to the gait phases. The details of model construction, learning, and evaluation processes are described below.

B. MODEL CONSTRUCTION

There are different types of HMM structures, such as the ergodic model [35] with all transitions between states enabled. The moving pattern of the prosthetic leg is one-way and the gait phase appears in the order of Toeoff, Midswing,

Heelstrike, Midstance during normal gait cycles. The leg movement also occurs in successive order inside each gait phase. Therefore, a typical left-to-right HMM without state skips as shown in **Fig.** 5 is constructed.

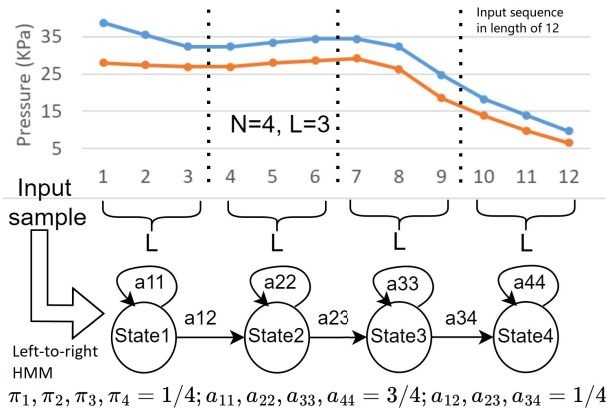

FIGURE 5. HMM model construction.

The first step in model construction is to determine the number of hidden states N and mixtures K, which is usually related to the corresponding physical significance in the patterns. In our case, since the gait cycle is already segmented in the dataset and each GMM-HMM represents one gait phase, the choice of N is determined by the length of the input pressure sequence. For example, if one input has three frames, its length is three, then N should be less or equal to three. For a statistically significant GMM-HMM, at least two hidden states are required. K depends on the observed feature distribution, which needs further search according to the input. Usually, it starts from two and ends when the accuracy rate is saturated. The observed data should be allocated to the hidden states in the model. In a left-to-right structure, uniform state assignment is preferred. The observed sequences are uniformly divided into N hidden states with length L per state, and the Gaussian mixture model takes place in each state. **Fig.** 5 shows an example of a constructed model taking the input sample in the length of 12 from the Midstance phase. When N is set to 4, L is 3 for each hidden state.

The second step is to initialize GMM-HMM parameters. As discussed in the previous section, the parameters are $\lambda = (\pi, A, g)$. π and A can be derived based on the initial alignment, where each element in π is $1/N$ and the state transition matrix A is calculated by dividing the number of transitions to other states by the total number of transitions, $a_{i,i} = L/(L+1)$ and $a_{i,i+1} = 1/(L+1)$. The initialized parameters from the example input are also given in **Fig.** 5. The GMM parameters g are initialized by the K-means clustering algorithm, which runs ten times to maximize the likelihood.

C. LEARNING PROCESS

After model construction, the learning process updates the initialized model parameters to realign closer to the real situation. The Viterbi training is applied. It records each possible state' s previous optimal path probability at each moment and the previous state of the optimal path simultaneously. Then it iterates backward continuously to find the state corresponding to the maximum probability value at the last time point and backtracks forward to get the optimal path. After that, the optimal state transition is also obtained. The transition probability A is updated according to the new allocation of observed sequences over the hidden states. g also changes with the updated mean and variance, which is used to calculate the emission probability B.

For each training iteration, this step is repeated, and new A, B can be obtained to perform the next Viterbi training. This loops until it reaches the desired iteration number, and then the learning process of GMM-HMM is completed.

D. EVALUATION PROCESS

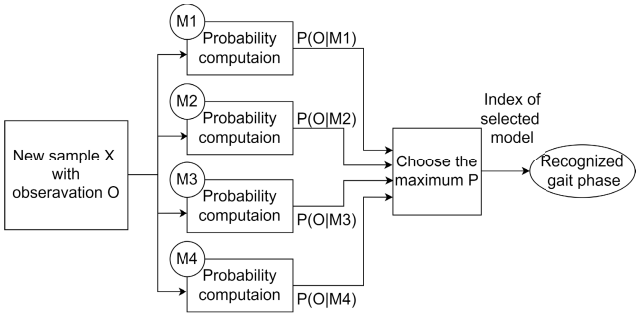

FIGURE 6. Gait phase labeling process.

The characteristics of pressure signals are statistically captured through the learning process. As **Fig.** 6 shows, the evaluation process works as an isolated phase recognizer centered after the four trained GMM-HMMs, where each represents a distinct gait phase. The pressure data from the test dataset are treated as feature vectors that reflect the movement of each gait phase. Based on the learned model parameters λ, the probability computation produces the probabilistic score of the input features against each GMM-HMM.

With the learned model M with parameter λ, and the new observation O from test sequences, Viterbi decoding [29] can uncover the hidden state sequence and find the emission probability $P(O|M)$ for each of four GMM-HMM models. The final choice of gait phase X is determined by **Eq.** (3),

$$X = argmax(P(O|M_1), P(O|M_2), P(O|M_3), P(O|M_4)) \quad (3)$$

where M_1 to M_4 represents GMM-HMM for gait phases 1 to 4. Eventually, the recognition decision is made on which output has the highest likelihood. Then these predicted gait phases are compared with ground truth to check the recognition rate.

VI. EVALUATION AND RESULTS

A. DATA COLLECTION AND EVALUATION SETUP

We use data acquired from a set of clinical trials to evaluate the performance of the proposed multiple GMM-HMM

approach. These clinical trials were conducted in hospitals in Spain and the UK. All trials were done with amputees after the trial protocols had been reviewed and approved by responsible national authorities[1,2]. The trial procedure was well defined as described in [14] before the actual trials with amputees. The trial datasets are archived at [36].

An embedded pressure-measuring system [14] using wearable QTSS™ (Quantum Technology Super Sensors) pressure sensors [37] is built for trials. Six human subjects with different profiles are involved (four males and two females; age: 58 ± 8 years; height: 174 ± 10 cm; weight: 73 ± 13 kg). All of them have transfemoral prostheses, four on the left side and two on the right side.

Pressure sensor strips are deployed on four edges inside the socket and perpendicular to the ground, including the anterior, posterior, medial, and lateral edges. The sensors on the strip are placed from the proximal end to the distal end in a fixed order with proper intervals to avoid overlapping.

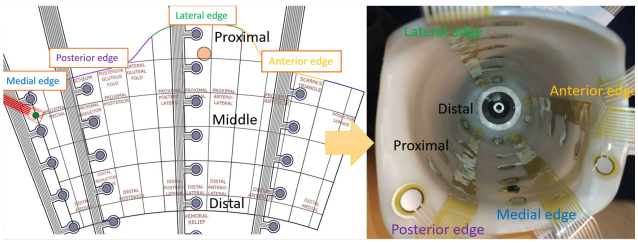

FIGURE 7. Sensor deployment map and placement in the socket.

The designed sensor layout schematic and the placement inside the socket are illustrated in **Fig.** 7, where the circles on the strips represent the sensing elements, and the labels indicate the region segmentation inside the socket.

Each subject wore their daily used socket and performed level ground walking for five minutes at their own speed. The measurement is taken at a rate of 20 Hz, which means 20 frames of sensor recordings per second. Besides the pressure data, there is an IMU mounted on the prosthetic leg. By aligning the timestamps of the IMU data and video recording of the tests, pressure data are labeled with corresponding gait phases, which are treated as the ground truth of our dataset. We can segment the pressure frames into gait phases based on these labels. The intra-socket pressure is pre-processed to contain only valid full gait cycles, during which irregular activities other than normal walking are removed, such as turning around at the end of the walking corridor or taking short rests between gait cycles. Note that for each phase we will keep at least two frames in order to maintain a meaningful number of hidden states. After that, we count the valid gait cycles for all subjects. There are 135, 194, 144, 102, 111, and 113 complete gait cycles for Subject 1 to Subject 6, respectively.

The dataset is formatted in a list of pressure feature files, each containing a gait phase in one gait cycle. Hence there are in total four times the number of the gait cycle of feature files for one subject. The number of sensors deployed is the number of possible features observed, which varies among subjects. The evaluation is performed in three scenarios.

1) For a single subject: Separate multiple GMM-HMM models are trained and tested on each subject. 50% of the data is used in training while the other 50% is used for testing.
2) For multiple subjects: One GMM-HMM model is evaluated for multiple subjects, where the subjects' data are combined, with the same train test ratio of 50%:50%.
3) For the unseen subject: One multiple-GMM-HMM model is trained by five subjects and evaluated on the leave-out subject. The training set is 70% of the five-subject dataset, and the test set is the whole leave-out dataset.

We use **accuracy on the test set** as the gait recognition metric, which is defined as the ratio of the number of correct gait phase labels to the total number of inputs.

B. EVALUATION IN SINGLE-SUBJECT SCENARIO

For each subject, the accuracy results of recognized gait phases are evaluated based on different training configurations. Since the length of observed sequences for each phase has a minimum number of two, the number of hidden states is set to 2 for all GMM-HMM models, and the learning iteration is set to 30. The dataset is randomly shuffled before training.

1) IMPACT OF SPATIAL SENSORS

In our measurement, one sensor strip is designed to hold at most 8 sensors (E1 to E8). However, the actual number of sensors deployed in the trial depends on the physical length of the subjects' sockets to avoid overlap in the bottom area.

The location of sensors is summarized in **Fig.** 8, where the unused sensors are marked with × . P means the proximal end, M means the middle region, and D means the distal end. We can count that Subject 1 has 25 sensors, Subject 2 has 15 sensors, Subject 3 has 24 sensors, Subject 4 has 22 sensors, Subject 5 has 21 sensors, and Subject 6 has 16 sensors inside the socket. For the sensor selection, since each subject has a different sensor layout in the trial, we consider two options. One is to use the common sensor positions among all subjects, which includes the top two sensors from the proximal end of each edge. Therefore $2 \times 4 = 8$ sensors are selected, whose positions are highlighted by the red box in **Fig.** 8. Another assumption is that all pressure sensors used in the trial are treated as valid features, though the sensors at the distal end have a much smaller pressure variation than others.

[1]Comité de Ética de la Investigación con medicamentos (CEIm) and Agencia Española de Medicamentos y Productos Sanitarios (AEMPS) approvals were obtained.

[2]Health Research Authority (HRA) and Medicines and Healthcare Products Regulatory Agency (MHRA) approvals were obtained (IRAS Project ID: 292614).

	Subject 1				Subject 2			
Strip	Anterior	Posterior	Medial	Lateral	Anterior	Posterior	Medial	Lateral
E8	P	P	P	P	P	P	P	P
E7	P	P	M	P	P	P	D	P
E6	M	M	M	P	D	M	X	P
E5	M	M	M	M	X	D	X	M
E4	M	M	D	M	X	X	X	M
E3	D	M	X	M	X	X	X	D
E2	X	D	X	D	X	X	X	X
E1	X	X	X	X	X	X	X	X
	Subject 3				Subject 4			
Strip	Anterior	Posterior	Medial	Lateral	Anterior	Posterior	Medial	Lateral
E8	P	P	P	P	P	P	P	P
E7	P	P	M	P	P	P	M	P
E6	M	M	M	P	M	M	M	P
E5	M	M	M	M	M	M	M	M
E4	M	M	D	M	D	D	D	M
E3	D	D	X	M	X	X	X	M
E2	X	X	X	D	X	X	X	D
E1	X	X	X	X	X	X	X	X
	Subject 5				Subject 6			
Strip	Anterior	Posterior	Medial	Lateral	Anterior	Posterior	Medial	Lateral
E8	P	P	P	P	P	P	P	P
E7	P	P	M	P	P	P	M	P
E6	M	M	M	P	M	M	D	P
E5	M	M	D	M	D	D	X	M
E4	D	D	X	M	X	X	X	D
E3	X	X	X	M	X	X	X	X
E2	X	X	X	D	X	X	X	X
E1	X	X	X	X	X	X	X	X

FIGURE 8. Sensor location for six human subjects.

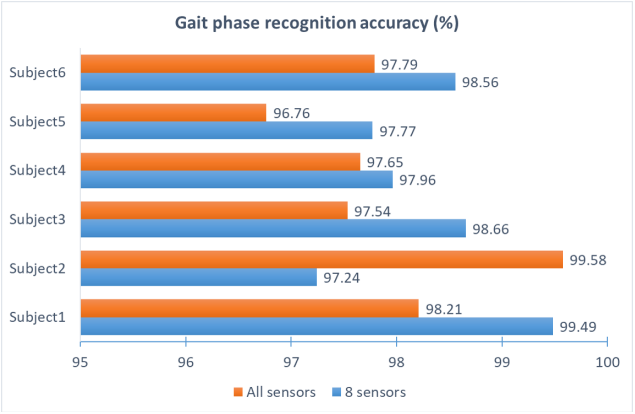

FIGURE 9. Average recognition accuracy (%) for selection on spatial sensors in single-subject scenario.

In this situation, we traverse the Gaussian mixtures K from 2 to 6 and take the average recognition accuracy on the test set as the result shown in **Fig.** 9. For Subjects 1, 3, 4, 5, and 6, the 8-sensor setup gives better accuracy of 1.1% and 1.3% respectively than the all-sensor. For Subject 2, the 8-sensor has less accuracy of 2.3% than the all-sensor situation. Generally, both configuration achieves a high recognition accuracy, and 8-sensor selection works better in most cases as it extracts the more significant pressure margin, which is usually on the proximal end. However, for Subject 2, since the socket has a much shorter length than others, the selected sensors are located down to the distal region for the medial edge. The pressure behavior is different from the other five subjects. In this case, the all-sensor selection is better for Subject 2.

2) SELECTION OF GAUSSIAN MIXTURES K

Besides the options for the spatial sensors, Gaussian mixtures can also affect the performance by finding a good fit for the input data. We choose the number of Gaussian mixtures K from 2 to 6 for evaluation and use the 8-sensor selection as a reference.

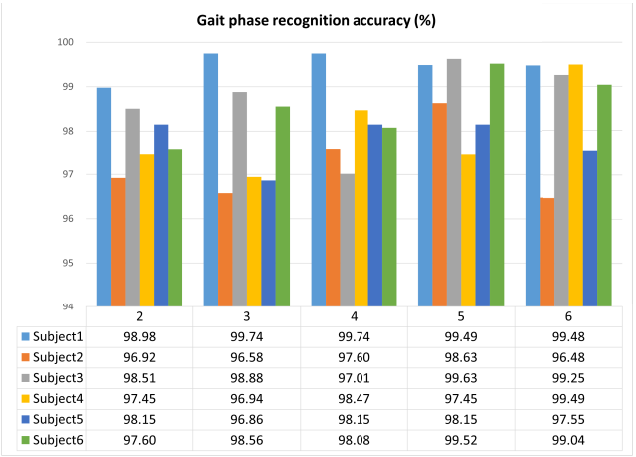

	2	3	4	5	6
Subject1	98.98	99.74	99.74	99.49	99.48
Subject2	96.92	96.58	97.60	98.63	96.48
Subject3	98.51	98.88	97.01	99.63	99.25
Subject4	97.45	96.94	98.47	97.45	99.49
Subject5	98.15	96.86	98.15	98.15	97.55
Subject6	97.60	98.56	98.08	99.52	99.04

FIGURE 10. Accuracy (%) for selection of Gaussian mixtures $K = 2$ to 6 in single-subject scenario.

Fig. 10 plots the recognition accuracy of different Gaussian mixtures K on six subjects over all four phases. We can observe that for Subject 1, K equals 3 and 4 have better accuracy than others. For Subjects 2, 3, and 6, $K = 5$ has the best results. For Subject 4, $K = 6$ has the highest accuracy. For Subject 5, K equals 4 and 5 have the same accuracy and are higher than other choices of the mixture number.

The proper choice of K depends on the actual data length and distribution. As all of the gait phase observation sequence lengths are less than 20, it is quite enough to use 4 to 5 Gaussian mixtures to fit the emission probability of HMM. When K is larger than 5, the accuracy starts to drop. The possible reason is overfitting, as the increased model flexibility may capture unexpected pressure fluctuation rather than the underlying relationship to the gait phase.

C. EVALUATION IN MULTIPLE-SUBJECT SCENARIO

Upon the single-subject scenario, we extend the gait phase recognition ability of the proposed multiple GMM-HMM method to multiple subjects. This examines the compatibility of our method with various amputees. From previous results, we consider the 8-sensor selection as the common feature. The total training set includes 400 gait cycles, and the test set includes 399 gait cycles.

Fig. 11 shows the gait phase recognition accuracy among six human subjects with Gaussian mixtures K from 2 to 6. We can observe that the model with two Gaussian mixtures is not enough to fit the data, which gives a lower recognition accuracy of 2% to 11% than the model with a higher number of mixtures. The 5-mixture model can achieve fairly good accuracy on the test set for around 97.4%. This aligns with

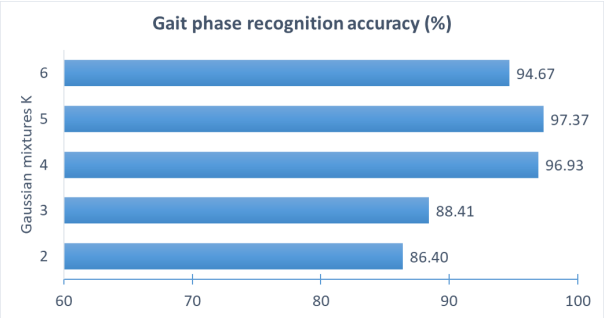

FIGURE 11. Accuracy (%) for selection of Gaussian mixtures $K = 2$ to 6 in multiple-subject scenario.

the observation in the single-subject scenario that $K = 5$ is a good choice for our interfacial pressure dataset.

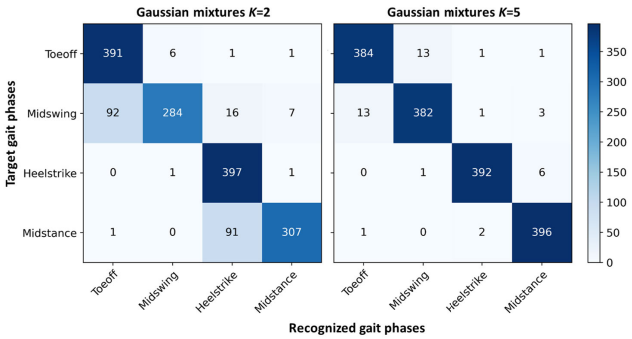

FIGURE 12. Confusion matrices for four gait phases with Gaussian mixtures $K = 2$ and $K = 5$.

To check the phase-wise accuracy, we plot the confusion matrix on recognition result for the multiple-subject scenario in **Fig.** 12. Here we show the proposed approach with the number of Gaussian mixtures $K = 2$ and $K = 5$.

From the $K = 2$ confusion matrix, we can see for Toeoff and Heelstrike phases, there are few recognition errors. While in the Midswing and Midstance phases, the recognition accuracy is relatively low for the 2-mixture model. There are around 23% of the testing samples in the Midswing phase are misclassified to the Toeoff phase. A similar amount of misclassifications also appear in the testing samples in the Midstance phase, which is predicted to be the Heelstrike phase. The possible reason is that when the training samples contain different human subjects, only two Gaussian mixtures per state are not enough to simulate the actual feature distribution. This can also explain why it behaves even worse in the multiple-subject scenario than in the single-subject scenario.

For the 5-mixture model, the confusion matrix shows good results with only 15 and 17 input samples misclassified for Toeoff and Midswing phases. For Heelstrike and Midstance phases, the recognition rate is 98.25% and 99.25%, respectively. Since the pressure change during the first two phases in a gait cycle is normally not as obvious as the other two phases, it's harder to distinguish them with the limited number of training observations.

D. EVALUATION IN UNSEEN-SUBJECT SCENARIO

To better investigate the generalization of the proposed method, a leave-one-subject-out validation is designed. As the results of the previous scenarios suggest, here we set the Gaussian mixture K to 5, and use the 8-sensor selection as the common feature. **Fig.** 13 shows the gait phase recognition accuracy on the leave-out subject evaluated on the GMM-HMM model trained from the other five subjects. Among the six cases, the best case is for subject 3, on which the model reaches a recognition accuracy of 84.55%.

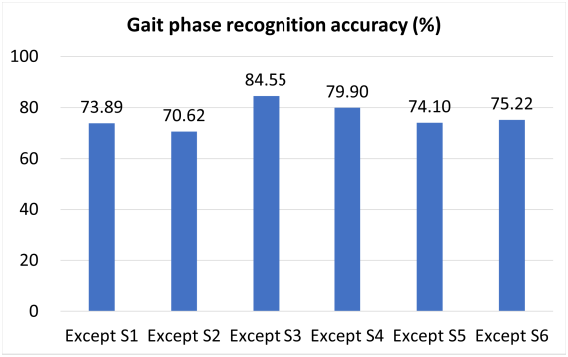

FIGURE 13. Accuracy (%) in unseen-subject scenario with Gaussian mixture $K = 5$ and 8-sensor.

The evaluation results on unseen subjects indicate that the proposed method has the ability for generalization, but the performance drops as the data distribution can vary a lot between trained and unseen subjects. The current model's capability is limited as the available number of subjects' data for training is small. The multiple-GMM-HMM can improve its generalizability by learning from more cases with diverse conditions.

E. SUMMARY

For the single-subject scenario, the supervised multiple GMM-HMM can reach around 99.5% recognition accuracy with proper parameter selection on the number of sensors and Gaussian mixtures. For the multiple-subject scenario, our approach can still maintain a high recognition accuracy of 97.37% with five Gaussian mixtures and an 8-sensor configuration. For the unseen-subject scenario, our model can reach an average of 76.38% recognition accuracy on the leave-out subject, which shows the potential for model generalization.

VII. COMPARISON OF THE PROPOSED APPROACH WITH WIDELY-USED RECOGNITION METHODS

In this section, we compare the performance of our multiple GMM-HMM approach with two well-known gait phase recognition methods, encompassing the unsupervised single GMM-HMM (CHMM) method [26], and the supervised LSTM model [22].

For the single GMM-HMM method, the model construction is similar to the multiple GMM-HMM approach. However, instead of employing separate models for distinct

gait phases, it represents all gait phases using one model, which means the four states in **Fig.** 5 are naturally linked with four physical gait phases. Therefore, it possesses the capability to discern gait phases throughout a complete gait cycle directly.

LSTM is a type of recurrent neural network model that is designed to extract time series data features for both short-term and long-term. Since the pressure sensor data are collected continuously when the subject walks with the artificial leg, the temporal pressure information can be extracted using the LSTM network. Then we can predict the next gait event based on the current pressure sequence.

A. RECOGNITION ACCURACY COMPARISON

We evaluate the same scenarios including the single-subject, multiple-subject, and unseen-subject using the single GMM-HMM and LSTM methods, and compare their gait phase recognition accuracy with our approach. For ease of comparison, we choose the 8-sensor situation for all scenarios. We use the same train-test ratio to evaluate these two methods as in our approach.

For the single GMM-HMM method, we segment the original dataset by gait cycles, and each gait cycle is treated as one input sequence. Since this method is unsupervised, we define the training process as updating model parameters according to the input. Then for the test process, the model parameters are fixed to label the gait phase for every data point in the input sequence. We have tried different selections of Gaussian mixtures K, and we found that here $K = 3$ performs the best. So we use this for all evaluations on the single GMM-HMM method.

The LSTM network consists of two LSTM layers and one fully connected layer. To construct the train set and test set for LSTM, we use a fixed-length sliding window as in [23] to generate multiple subsequences from the whole walking series. The window size is set to 20, which is aligned with the pressure sensor sampling frequency of 20 Hz. The sliding step is one as we execute a one-step prediction immediately after the input subsequence. We set 64 hidden neurons in each LSTM layer and one output neuron for the fully connected layer. The final output of the last fully connected layer is rounded to represent the gait phase associated with the input sample. The model is trained with a batch size of 64 for 5 epochs on the single subject scenario and trained for 10 epochs on the other two scenarios.

Tab. 1 summarize the evaluation results for all three scenarios using these recognition methods. For the single-subject scenario, our approach outperforms the single GMM-HMM and LSTM by 46.1% and 14.8% on average in terms of gait phase recognition accuracy. In the multiple-subject context, despite observing a decrease in the overall accuracy when contrasted with the single-subject scenario, the multiple GMM-HMM approach still yields superior performance than the single GMM-HMM and LSTM by 44.5% and 15.7% of accuracy respectively. In the context of unseen subjects, both LSTM and our approach demonstrate comparable accuracy, with an average of 76%. The single GMM-HMM method shows notably inferior accuracy results than these two methods. Therefore, the performance of our multiple GMM-HMM approach is better than the unsupervised single GMM-HMM method in all evaluated situations. Compared with the supervised LSTM model, the proposed approach is better in single-subject and multiple-subject scenarios, while remaining competitive in the unseen-subject tests.

TABLE 1. Gait phase recognition accuracy comparison.

Scenarios	Subject	Gait phase recognition accuracy (%)		
		Multiple GMM-HMM (Ours)	Single GMM-HMM [26]	LSTM [22]
A: Single subject	S1	99.49	59.41	85.28
	S2	97.24	50.17	90.57
	S3	98.66	42.22	84.65
	S4	97.96	49.87	81.47
	S5	97.77	58.52	73.85
	S6	98.56	52.98	85.00
	Average	98.28	52.20	83.47
B: Multiple subject	All	92.76	48.30	77.10
C: Unseen subject	Ex. S1	73.89	66.67	75.28
	Ex. S2	70.62	50.16	77.38
	Ex. S3	84.55	56.16	82.34
	Ex. S4	79.90	57.23	80.99
	Ex. S5	74.10	44.76	60.25
	Ex. S6	75.22	69.86	80.28
	Average	76.38	57.47	76.09

B. MODEL COMPLEXITY COMPARISON

Besides the model recognition performance, the model complexity is also a concern for its implementation on embedded platforms. Many applications for accurate amputee gait phase recognition such as exoskeleton movement control [10] and automatic prosthesis socket size adjustment [11], [12], in which real-time recognition is preferred. Here we discuss the inference computation complexity and model size of our approach and the aforementioned recognition methods.

For the single GMM-HMM model, the inference time complexity can be written as $O(TNK + TN^2)$, where T is the length of the input sequence, N is the number of hidden states, and K is the number of Gaussian mixtures. N, K can be treated as constants, for example, $N = 4, K = 3$. So its execution time grows linear with the input sequence length T.

Since the proposed multiple GMM-HMM approach is a combination of n single GMM-HMM models with a comparator at the end, the computation complexity can be approximated as $O(n \times (TNK + TN^2))$. In our case, n equals 4 as there are four gait phases to recognize. In the multiple GMM-HMM approach, T represents the length of one gait phase instead of the whole gait cycle, which is smaller than that in the single GMM-HMM method, and typically in the range of 5 to 20. Therefore, our approach also has the linear time complexity to the input sequence length T, and the actual

computation time is slightly larger than the single GMM-HMM.

On the other hand, the LSTM method requires $O(TH^2)$, where T is the length of the input sequence, and H is the number of neurons in the LSTM layer. Normally, H is much larger than N, for example, we have $T = 20$ and use $H = 64$ in our evaluation. Moreover, our complete LSTM model comprises two LSTM layers and one fully connected layer, which largely increases the computation time. So regarding the inference time, GMM-HMM-based methods are more efficient than the LSTM method.

To compare the model size, we count the model parameters for three methods. In the single GMM-HMM model, the total number of parameters is $N^2 + K \times (1 + D + D^2)$, where N, K represents the states and Gaussian mixtures, and D is the dimensions of the input data. Considering the 8-sensor situation, we have the model size of $4^2 + 3 \times (1 + 8 + 8^2) = 235$ parameters. Similarly, we can calculate the model size of our multiple GMM-HMM approach as 940 parameters when we keep the same N, K, and D.

For the LSTM model, the first LSTM layer comprises $4 \times (64 + 8) \times 64 = 18432$ weights and 256 biases, totaling 18688 parameters. The second LSTM layer consists of 33024 parameters and the fully connected layer has 65 parameters. Thus, the entire LSTM model encompasses 51777 parameters, whose size is 55 times larger than that of the proposed multiple GMM-HMM approach.

In this case, our multiple GMM-HMM approach has better model complexity regarding both gait recognition time and model size than the LSTM approach. Though it requires more computation time and storage than the single GMM-HMM method, the enlarged resources are affordable for most embedded devices, while the gait phase recognition accuracy can be improved a lot.

VIII. CONCLUSION

In this paper, we present the multiple GMM-HMM approach for lower limb amputee gait phase recognition based on the intra-socket pressure measurement. The proposed method can learn the gait pattern from interfacial pressure features collected by wearable sensors. It is validated on a dataset containing six human subjects. The choice of model parameters is discussed to improve the accuracy of recognition. The evaluation results on the trained models show satisfying accuracy. Relatively good recognition accuracy for leave-one-out validation proves the generalization ability of our method. The multiple GMM-HMM approach shows superior recognition accuracy in all scenarios when compared to the single GMM-HMM method, and in single-subject and multiple-subject scenarios compared to LSTM. Our approach requires much fewer computation resources but still maintains recognition accuracy advantages in the context of unseen subjects compared with the LSTM method.

Our future work aims to integrate the recognition process in gait analysis for comfort socket design. One essential step is automatic gait recognition on edge devices in real-time. Also, more subjects could be included to support the general applicability and further extend the recognition ability of the proposed approach.

ACKNOWLEDGMENT

The clinical trial subject data such as age, height, weight, and intra-socket pressure were provided by the South Tees Hospitals NHS Foundation Trust, U.K., and Servicio Andaluz de Salud, Spain, within the SocketSense project (https://www.socketsense.eu).

REFERENCES

[1] L. Paternò, M. Ibrahimi, E. Gruppioni, A. Menciassi, and L. Ricotti, "Sockets for limb prostheses: A review of existing technologies and open challenges," *IEEE Trans. Biomed. Eng.*, vol. 65, no. 9, pp. 1996–2010, Sep. 2018.

[2] S.-T. Ko, F. Asplund, and B. Zeybek, "A scoping review of pressure measurements in prosthetic sockets of transfemoral amputees during ambulation: Key considerations for sensor design," *Sensors*, vol. 21, no. 15, p. 5016, Jul. 2021.

[3] D. Chen, P. Su, S. Ottikkutti, P. Vartholomeos, K. N. Tahmasebi, and M. Karamousadakis, "Analyzing dynamic operational conditions of limb prosthetic sockets with a mechatronics-twin framework," *Appl. Sci.*, vol. 12, no. 3, p. 986, Jan. 2022.

[4] D. Dong, C. Ma, M. Wang, H. T. Vu, B. Vanderborght, and Y. Sun, "A low-cost framework for the recognition of human motion gait phases and patterns based on multi-source perception fusion," *Eng. Appl. Artif. Intell.*, vol. 120, Apr. 2023, Art. no. 105886.

[5] T. Lencioni, I. Carpinella, M. Rabuffetti, A. Marzegan, and M. Ferrarin, "Human kinematic, kinetic and EMG data during different walking and stair ascending and descending tasks," *Sci. Data*, vol. 6, no. 1, p. 309, Dec. 2019.

[6] U. Trinler, K. Hollands, R. Jones, and R. Baker, "A systematic review of approaches to modelling lower limb muscle forces during gait: Applicability to clinical gait analyses," *Gait Posture*, vol. 61, pp. 353–361, Mar. 2018.

[7] Z. Zhu, P. Su, S. Zhong, J. Huang, S. Ottikkutti, K. N. Tahmasebi, Z. Zou, L. Zheng, and D. Chen, "Using a VAE-SOM architecture for anomaly detection of flexible sensors in limb prosthesis," *J. Ind. Inf. Integr.*, vol. 35, Oct. 2023, Art. no. 100490.

[8] T. Yan, M. Cempini, C. M. Oddo, and N. Vitiello, "Review of assistive strategies in powered lower-limb orthoses and exoskeletons," *Robot. Auto. Syst.*, vol. 64, pp. 120–136, Feb. 2015.

[9] B. Kalita, J. Narayan, and S. K. Dwivedy, "Development of active lower limb robotic-based orthosis and exoskeleton devices: A systematic review," *Int. J. Social Robot.*, vol. 13, no. 4, pp. 775–793, Jul. 2021.

[10] M. K. Ishmael, D. Archangeli, and T. Lenzi, "Powered hip exoskeleton improves walking economy in individuals with above-knee amputation," *Nature Med.*, vol. 27, no. 10, pp. 1783–1788, Oct. 2021.

[11] E. J. Weathersby, J. L. Garbini, B. G. Larsen, J. B. McLean, A. C. Vamos, and J. E. Sanders, "Automatic control of prosthetic socket size for people WithTranstibial amputation: Implementation and evaluation," *IEEE Trans. Biomed. Eng.*, vol. 68, no. 1, pp. 36–46, Jan. 2021.

[12] J.-H. Seo, H.-J. Lee, D.-W. Seo, D.-K. Lee, O.-W. Kwon, M.-K. Kwak, and K.-H. Lee, "A prosthetic socket with active volume compensation for amputated lower limb," *Sensors*, vol. 21, no. 2, p. 407, Jan. 2021.

[13] H. T. T. Vu, D. Dong, H.-L. Cao, T. Verstraten, D. Lefeber, B. Vanderborght, and J. Geeroms, "A review of gait phase detection algorithms for lower limb prostheses," *Sensors*, vol. 20, no. 14, p. 3972, Jul. 2020.

[14] Z. Lu, W. Zhu, Y. Chen, J. Charnley, V. Dejke, A. Pomazanskyi, S.-T. Ko, B. Zeybek, P. Mehryar, Z. Ali, M. Karamousadakis, and D. Chen, "Wearable pressure sensing for lower limb amputees," in *Proc. IEEE Biomed. Circuits Syst. Conf. (BioCAS)*, Oct. 2022, pp. 105–109.

[15] A. Esquenazi, "Gait analysis in lower-limb amputation and prosthetic rehabilitation," *Phys. Med. Rehabil. Clinics North Amer.*, vol. 25, no. 1, pp. 153–167, Feb. 2014.

[16] S. C. Henao, C. Orozco, and J. Ramírez, "Influence of gait cycle loads on stress distribution at the residual limb/socket interface of transfemoral amputees: A finite element analysis," *Sci. Rep.*, vol. 10, no. 1, pp. 1–11, Mar. 2020.
[17] W. Carrigan, C. Nothnagle, P. Savant, F. Gao, and M. B. J. Wijesundara, "Pneumatic actuator inserts for interface pressure mapping and fit improvement in lower extremity prosthetics," in *Proc. 6th IEEE Int. Conf. Biomed. Robot. Biomechatronics (BioRob)*, Jun. 2016, pp. 574–579.
[18] R. Baud, A. R. Manzoori, A. Ijspeert, and M. Bouri, "Review of control strategies for lower-limb exoskeletons to assist gait," *J. NeuroEng. Rehabil.*, vol. 18, no. 1, pp. 1–34, Dec. 2021.
[19] S. Khandelwal and N. Wickström, "Gait event detection in real-world environment for long-term applications: Incorporating domain knowledge into time-frequency analysis," *IEEE Trans. Neural Syst. Rehabil. Eng.*, vol. 24, no. 12, pp. 1363–1372, Dec. 2016.
[20] H. F. Maqbool, M. A. B. Husman, M. I. Awad, A. Abouhossein, N. Iqbal, M. Tahir, and A. A. Dehghani-Sanij, "Heuristic real-time detection of temporal gait events for lower limb amputees," *IEEE Sensors J.*, vol. 19, no. 8, pp. 3138–3148, Apr. 2019.
[21] S. Cai, D. Chen, B. Fan, M. Du, G. Bao, and G. Li, "Gait phases recognition based on lower limb sEMG signals using LDA-PSO-LSTM algorithm," *Biomed. Signal Process. Control*, vol. 80, Feb. 2023, Art. no. 104272.
[22] Z. Ding, C. Yang, K. Xing, X. Ma, K. Yang, H. Guo, C. Yi, and F. Jiang, "The real time gait phase detection based on long short-term memory," in *Proc. IEEE 3rd Int. Conf. Data Sci. Cyberspace (DSC)*, Jun. 2018, pp. 33–38.
[23] L. Tran, T. Hoang, T. Nguyen, H. Kim, and D. Choi, "Multi-model long short-term memory network for gait recognition using window-based data segment," *IEEE Access*, vol. 9, pp. 23826–23839, 2021.
[24] M. Sarshar, S. Polturi, and L. Schega, "Gait phase estimation by using LSTM in IMU-based gait analysis—Proof of concept," *Sensors*, vol. 21, no. 17, p. 5749, Aug. 2021.
[25] F. Attal, Y. Amirat, A. Chibani, and S. Mohammed, "Automatic recognition of gait phases using a multiple-regression hidden Markov model," *IEEE/ASME Trans. Mechatronics*, vol. 23, no. 4, pp. 1597–1607, Aug. 2018.
[26] F. Attal, Y. Amirat, A. Chibani, and S. Mohammed, "Human gait phase recognition using a hidden Markov model framework," in *Proc. IEEE/RSJ Int. Conf. Intell. Robots Syst. (IROS)*, Oct. 2020, pp. 10299–10304.
[27] J. Yang, J. Pan, and J. Li, "SEMG-based continuous hand gesture recognition using GMM-HMM and threshold model," in *Proc. IEEE Int. Conf. Robot. Biomimetics (ROBIO)*, Dec. 2017, pp. 1509–1514.
[28] X. Cheng, B. Huang, and J. Zong, "Device-free human activity recognition based on GMM-HMM using channel state information," *IEEE Access*, vol. 9, pp. 76592–76601, 2021.
[29] L. R. Rabiner, "A tutorial on hidden Markov models and selected applications in speech recognition," *Proc. IEEE*, vol. 77, no. 2, pp. 257–286, 1989.
[30] Y. Ephraim and N. Merhav, "Hidden Markov processes," *IEEE Trans. Inf. Theory*, vol. 48, no. 6, pp. 1518–1569, Jun. 2002.
[31] A. E. Allahverdyan and A. Galstyan, "Comparative analysis of Viterbi training and maximum likelihood estimation for HMMs," in *Proc. Adv. Neural Inf. Process. Syst.*, vol. 24, Dec. 2011, pp. 1674–1682.
[32] M. Franzini, K.-F. Lee, and A. Waibel, "Connectionist Viterbi training: A new hybrid method for continuous speech recognition," in *Proc. Int. Conf. Acoust., Speech, Signal Process.*, 1990, pp. 425–428.
[33] J. Taborri, E. Palermo, S. Rossi, and P. Cappa, "Gait partitioning methods: A systematic review," *Sensors*, vol. 16, no. 1, p. 66, Jan. 2016.
[34] T. Castermans, M. Duvinage, G. Cheron, and T. Dutoit, "Towards effective non-invasive brain–computer interfaces dedicated to gait rehabilitation systems," *Brain Sci.*, vol. 4, no. 1, pp. 1–48, Dec. 2013.
[35] S. A. S. Kumar and V. Ramasubramanian, "Automatic language identification using ergodic-HMM," in *Proc. IEEE Int. Conf. Acoust., Speech, Signal Process.*, vol. 1, Mar. 2005, pp. 609–612.
[36] SocketSense Consortium, "SocketSense open access data," Zenodo, Dec. 2022, doi: 10.5281/zenodo.7400478.
[37] V. Dejke, M. P. Eng, K. Brinkfeldt, J. Charnley, D. Lussey, and C. Lussey, "Development of prototype low-cost QTSS™ wearable flexible more enviro-friendly pressure, shear, and friction sensors for dynamic prosthetic fit monitoring," *Sensors*, vol. 21, no. 11, p. 3764, May 2021.

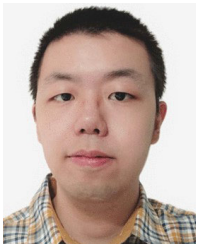

WENYAO ZHU (Graduate Student Member, IEEE) received the B.S. degree in electrical and computer engineering from Shanghai Jiao Tong University, China, in 2018, and the M.S. degree in embedded systems from the KTH Royal Institute of Technology, Sweden, in 2020. He is currently pursuing the Ph.D. degree with the Division of Electronics and Embedded Systems, School of Electrical Engineering and Computer Science, KTH Royal Institute of Technology. His research interests include hardware accelerators for AI, network-on-chip, edge computing, and embedded sensor systems.

ZHENBANG LIU received the B.S. degree in electrical engineering from Xi'an Jiaotong-Liverpool University, in 2019, and the dual M.S. degree in embedded systems from the Technical University of Berlin, Berlin, Germany, and the KTH Royal Institute of Technology, Stockholm, Sweden, in 2021. He is currently a Software Engineer in the field of automatic driving and intelligent manufacturing. His current research interests include automatic driving and digital industry algorithms.

YIZHI CHEN received the B.E. degree in electronic and information engineering from Wuhan University, China, in 2017, and the M.S. degree in communication and information technology from the University of Bremen, Germany, in 2021. He is currently pursuing the Ph.D. degree with the Division of Electronics and Embedded Systems, Department of Electrical Engineering, School of Electrical Engineering and Computer Science, KTH Royal Institute of Technology. His research interests include hardware accelerators for ML, computer architecture, network-on-chip, and fault-tolerant hardware for neural networks.

DEJIU CHEN (Senior Member, IEEE) was a Senior Technical Instructor with Enea Data AB, Sweden, from 2007 to 2009. He is currently a Docent (Principal Ph.D. Supervisor) and an Associate Professor of embedded control systems with the KTH Royal Institute of Technology, Sweden. He was a PI of the EU H2020 Research Project SocketSense on AI centric medical IoT. His research interests include engineering methods and tools, architecture design, safety engineering, and the design of self-X properties for optimal operation and lifecycle management of various cyber-physical systems.

ZHONGHAI LU (Senior Member, IEEE) received the B.S. degree in radio and electronics from Beijing Normal University, Beijing, China, in 1989, and the M.S. degree in system-on-chip design and the Ph.D. degree in electronic and computer system design from the KTH Royal Institute of Technology, Stockholm, Sweden, in 2002 and 2007, respectively. He was an Engineer in the area of electronic and embedded systems, from 1989 to 2000. He is currently a Professor with the School of Electrical Engineering and Computer Science, KTH Royal Institute of Technology. He has authored more than 200 peer-reviewed articles. His current research interests include AI for embedded systems, AI hardware, computer architecture, and electronic design automation.